The impact of thermally pulsing asymptotic giant branch stars on hierarchical galaxy formation models

Chiara Tonini,[1]★ Claudia Maraston,[1] Julien Devriendt,[2] Daniel Thomas[1] and Joseph Silk[2]

[1]*Institute of Cosmology and Gravitation, University of Portsmouth, Portsmouth PO1 3FX*
[2]*University of Oxford, Oxford OX1 3PU*

ABSTRACT

The spectro-photometric properties of galaxies in galaxy formation models are obtained by combining the predicted history of star formation and mass accretion with the physics of stellar evolution through stellar population models. In the recent literature, significant differences have emerged regarding the implementation of the thermally pulsing asymptotic giant branch phase of stellar evolution. The emission in the TP-AGB phase dominates the bolometric and near-IR spectrum of intermediate-age ($\sim$1 Gyr) stellar populations, hence it is crucial for the correct modelling of the galaxy luminosities and colours. In this paper, for the first time, we incorporate a full prescription of the TP-AGB phase in a semi-analytic model of galaxy formation. We find that the inclusion of the TP-AGB in the model spectra dramatically alters the predicted colour–magnitude relation and its evolution with redshift. When the TP-AGB phase is active, the rest-frame $V - K$ galaxy colours are redder by almost 2 mag in the redshift range $z \sim 2$–3 and by 1 mag at $z \sim 1$. Very red colours are produced in disc galaxies, so that the $V - K$ colour distributions of disc and spheroids are virtually undistinguishable at low redshifts. We also find that the galaxy K-band emission is more than 1 mag higher in the range $z \sim 1$–3. This may alleviate the difficulties met by the hierarchical clustering scenario in predicting the red galaxy population at high redshifts. The comparison between simulations and observations has to be revisited in the light of our results.

Key words: galaxies: evolution – galaxies: formation – galaxies: fundamental parameters – galaxies: high-redshift – galaxies: photometry.

1 INTRODUCTION

The modern theory of the formation and evolution of galaxies is built on the cold dark matter (CDM) hierarchical structure formation paradigm, and is supported by two powerful tools, semi-analytic models and smoothed particle hydrodynamic (SPH) simulations. In both cases, they combine the results of *N*-body simulations, producing the assembly of dark matter structures, with the baryonic physics describing cooling, star formation, feedback, chemical enrichment and dynamical interactions. The interface between models and observations is mainly constituted by the galaxy spectra, which can be modelled and interpreted to infer mass, age, chemical composition, star formation rate (SFR) and mass assembly history of the galaxy populations (see Baugh 2006 for a recent review).

The spectra of galaxies are obtained using stellar population models that predict the spectral energy distribution (SED) of ensembles of stars as a function of age, metallicity and the initial mass function (IMF). At any given galaxy age, the predicted emitted spectrum is a superposition of the synthetic spectra of the single stellar populations (SSPs) that compose the total stellar mass, assembled according to the model's SFR as a function of time.

Stellar population models currently used in published galaxy formation models and SPH simulations include Bruzual & Charlot (2003; adopted by Menci et al. 2005; Nagamine et al. 2005; Bower et al. 2006; Croton et al. 2006; De Lucia et al. 2006; Khochfar et al. 2007; Naab et al. 2007; Somerville et al. 2008), GRAphite and SILicate (GRASIL) by Silva et al. (1998; e.g. Granato et al. 2004; Monaco, Fontanot & Taffoni 2007), STARDUST by Devriendt, Guiderdoni & Sadat (1999; see Hatton et al. 2003) and Projet d'Etude des GAlaxies par Synthèse Évolutive (PEGASE) by Fioc & Rocca-Volmerange (1997; see Cattaneo et al. 2005; Mori & Umemura 2006). These stellar population models make use of the Padova (1994) stellar evolutionary tracks, which do not include the full contribution of the thermally pulsing asymptotic giant branch phase, as pointed out by Maraston (1998, 2005, hereafter M05) and more recently by other authors (e.g. Bruzual 2007; Marigo & Girardi 2007; Conroy, Gunn & White 2008; Eminian et al. 2008). As shown in Maraston (1998) and M05, the TP-AGB can account for up to 40 per cent of the bolometric light and 80 per cent of the light in the

★E-mail: chiara.tonini@port.ac.uk

K band. Hence, the neglect of this phase in the galaxy formation models leads to an underestimation of the flux redwards of 5000 Å, with a major effect in the near-IR.

The emission in this phase is significant for the stars in the mass range 2–3 M$_\odot$, and therefore peaks in a very short period of the life of the SSP, around the age of ~1 Gyr. For this reason, the TP-AGB light is a powerful marker of an intermediate-age stellar population and dominates the *K*-band luminosity in the post-starburst phases of star formation. Since the rest of the emission in the *K* band is contributed by old and/or metal-rich low-mass stars, the inclusion of the TP-AGB stars on top of the *K*-band background leads to dramatic differences in the colours and the mass–luminosity relation of model galaxies, especially in the early phases of their evolution.

To quantify the effect of the TP-AGB emission on the predicted galaxy colours at different redshifts, we run a semi-analytical code with different input SSPs, the M05 models (with TP-AGB) and the PEGASE models (without TP-AGB), and study the evolution of the colour–magnitude relation. For the scope of this paper, the PEGASE and the Bruzual & Charlot model SSPs are equivalent, since they are based on the same input physics. In particular, they make use of the same stellar evolutionary tracks (Padova tracks) and they employ the isochrone synthesis modelling, producing very similar SSP spectra (see M05 for an extended discussion on the properties of these models). We use GalICS as our reference semi-analytical model, set with standard ΛCDM cosmology and default astrophysical parameters. The model includes chemical enrichment and metallicity evolution based on the instantaneous recycling approximation (for details on the GalICS recipe see Hatton et al. 2003). We adopt no reddening by dust, to better isolate the TP-AGB effect. Between the runs, we do not vary the input physics except for the different SSP models. The results presented here do not depend, in essence, on the particular galaxy formation model, and can be applied to any other model based on CDM hierarchical clustering (see Discussion).

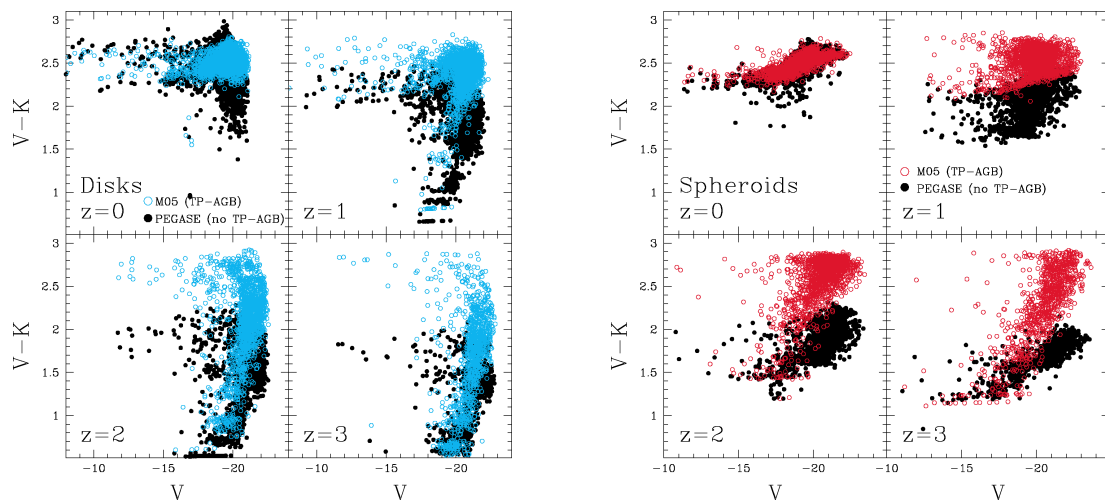## 2 THE PREDICTED COLOUR–MAGNITUDE RELATION

The evolution of a galaxy population manifests itself in the colour–magnitude relation as a function of redshift. The ageing of the stellar populations, the trend of the SFR with time, the metal enrichment, the mass accretion history and the morphology evolution produce changes in the galaxy spectra and hence in luminosities and colours. In our two test runs, the different SSP models are expected to produce different colour distributions, around the epoch when the contribution of the TP-AGB phase to the total emission is maximal. This is the case when either all the stellar populations are young, or anytime the SFR is high enough to provide new stellar populations which, by crossing the critical age range, overshadow the background MS and red giant branch (RGB) stars in the near-IR with TP-AGB stars.

Fig. 1 shows the rest-frame $V - K$ colour versus the optical V magnitude, for four different redshifts between $z = 0$ and 3, for the two test runs. The blue/red empty dots represent the M05 run, the black filled represents dots the PEGASE, the left-hand panel shows the disc population, the right-hand panel selects the spheroids population, which includes ellipticals and the bulges of spirals. For the present scope, the distinctive feature of these two types of objects is the star formation. In discs, the star formation follows the cooling of gas and the SFR is a function of the gas mass accretion rate and density. Spheroids do not directly receive cool gas and form via secular evolution from discs or via mergers, and in both cases star formation occurs in bursts.

Fig. 1 shows an impressive offset between the two runs. At $z = 3$, the TP-AGB emission in the M05 run produces a reddening of $V - K$ of up to 2 mag, and introduces a spread between the blue and the red end of the colour distribution much wider than the PEGASE. The distinctive feature of the effect is its dependence with redshift, caused by the evolution of the SFR in the model. While at $z = 1$ the offset in the colours is still significant, for lower redshifts it tends to disappear, mirroring the ageing of the stellar populations and the fading of the TP-AGB emission into the background IR produced by the MS and RGB stars (see M05).

An even larger offset between the M05 and PEGASE runs is shown in the spheroids case (right-hand panel). At $z = 3$, the two colour distributions meet only at the faint blue end, while the M05 steeper slope moves the rest of the objects redwards. The offset here is more dramatic and shows a trend with mass, with the most massive galaxies being more affected. This mirrors the fact that the star formation is more intense in massive objects, which undergo

Figure 1. The colour–magnitude relation $V - K$ versus V, at redshifts from $z = 0$ to 3, for discs (left-hand panel) and spheroids (right-hand panel) in a sub-sample of the GalICS simulation box [for clarity, a fraction (1/20) of the total output is plotted]; black filled dots show the PEGASE run, while blue/red empty dots show the M05 run. The sample is not complete in magnitude, due to the finite mass resolution of the GalICS *N*-body simulation (see Hatton et al. 2003 for details). Here, the stellar mass range is $2.3e5 \, M_\odot < M_{disc} < 4.5e11 \, M_\odot$ and $4.6e5 \, M_\odot < M_{SPH} < 4.5e11 \, M_\odot$, respectively.

a higher number of mergers accompanied by bursts. These events leave no gas available for residual star formation, and the massive new stellar populations soon turn into the AGB phase. The spheroids are soon dominated by the post-starburst phase, thus maximizing the impact of the red colours. In comparison, discs are bluer than spheroids for a given *V*-band luminosity and redshift, because of the continuous star formation triggered by gas infall, that somewhat dilutes the TP-AGB emission. In fact, very young stellar populations are barely affected by the TP-AGB emission, as already pointed out in Swinbank et al. (2008).

As expected, the offset decreases as the stellar populations grow old. The evolution of the PEGASE colours moves the galaxies from the blue to the red end at $z = 0$, but at high redshifts the PEGASE run predicts no red objects. On the contrary, the M05 run shows a continuous occupation of the red end, which at high redshifts is contributed by the young populations rich in TP-AGB stars, and at low redshift converges to the PEGASE due to the old age of the galaxies.

It is interesting to compare the M05 and the PEGASE runs in the $B - V$ colours, as is shown in Fig. 2. These spectral bands are insensitive to the TP-AGB emission, and in fact the two colour dis-tributions are now very similar. This highlights the main difference between the two runs. It is evident that, at any given redshift, an object in the M05 run can be very blue in $B - V$ and very red in $V - K$, while in the PEGASE run the $V - K$ colours show the same trend as the $B - V$. This is because, in the M05 run, $V - K$ red colours are not associated just with old quiescent galaxies, but are produced also by young objects if the TP-AGB phase is active. Note, for instance, the blue cloud in $B - V$ at $z = 0 - 1$ for discs. In the correspondent $V - K$ plot, these galaxies are very red in the M05 run because of TP-AGB stars, and the resulting colours are virtually undistin-guishable from those of spheroids on the red sequence. This is a remarkable result that will be subject to future investigation.

Fig. 3 portrays the distribution of the $V - K$ colour of discs and spheroids for about half of the total galaxy population in the simu-lation box ($\sim$23 000 galaxies at $z = 0$), for the M05 (blue/red) and PEGASE (black) runs. In the case of spheroids (right-hand panel), the two distributions are completely segregated at high redshift, with an offset of 2 mag in $V - K$. At $z = 1$, the offset is still of the order of unity, and disappears at later times. For the discs (left-hand panel), the distributions feature a larger spread and an offset of the order of unity down to $z = 1$, and converge at later times. Fig. 3
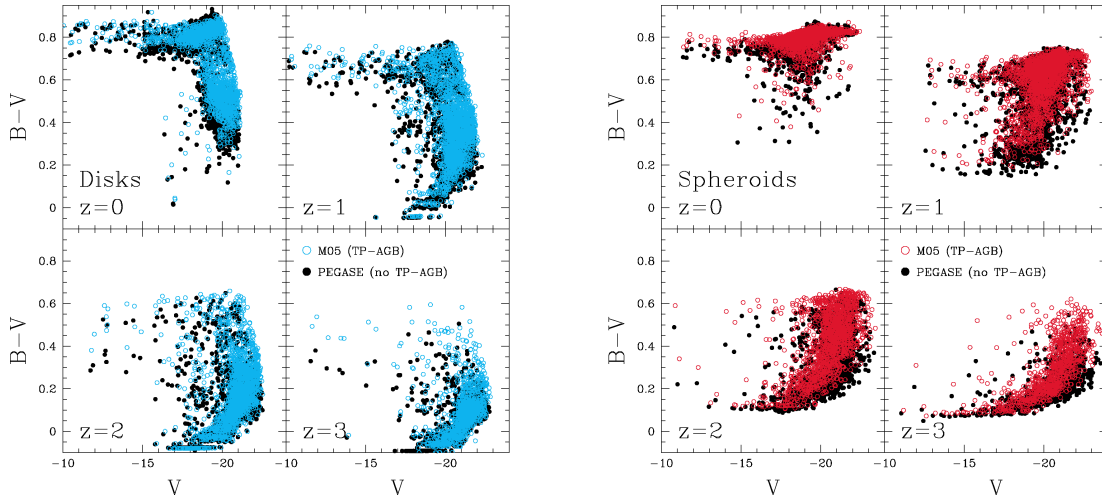
Figure 2. The colour–magnitude relation $B - V$ versus V, colour coding as in Fig. 1.
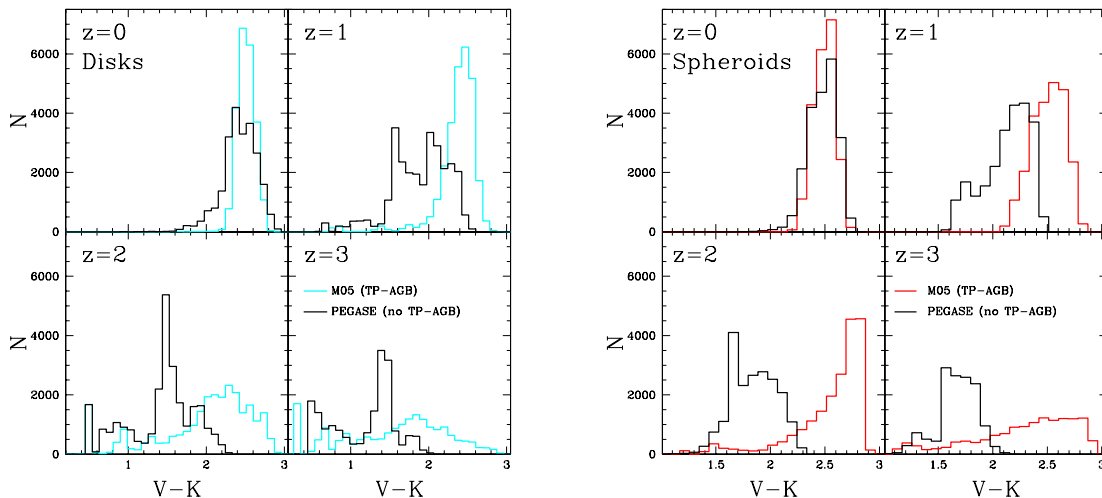
Figure 3. Histogram of the $V - K$ colour distribution for discs and spheroids, for half the GalICS population ($\sim$23 000 galaxies at $z = 0$), colour-coded as in Fig. 1.
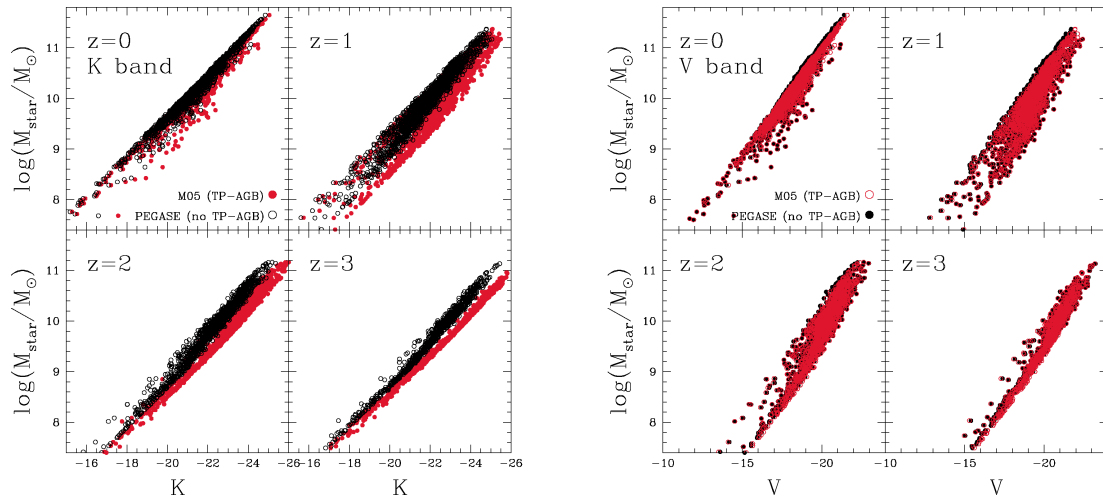
Figure 4. The *K*-band (left-hand panel) and *V*-band (right-hand panel) stellar mass versus luminosity relation for the spheroids population, at redshifts from $z = 0$ to 3 (remnants are taken into account in the stellar mass budget); colour-coding as in Fig. 1.

highlights the different colour evolution of the galaxies in the two runs. With respect to the M05, the PEGASE run lacks red young galaxies, and is overall bluer at every redshift. The TP-AGB emission makes the high-redshift M05 galaxies very red, and its effects are still dominant in $V - K$ down to $z = 1$. At the same time, the TP-AGB tends to counterbalance a bit of blue light, so that the M05 distribution is overall more sharply peaked.

3 THE LUMINOSITY–MASS RELATION

When the TP-AGB emission is not taken into account, the total stellar emission in the *K* band is contributed by low-mass MS stars and RGB stars with a lifespan of more than 10 Gyr. The correct disentanglement of the TP-AGB from this component severely affects the estimate of the M/L ratio, and is crucial when the *K*-band luminosity is used as a tracer of the galaxy mass. In Fig. 4 (left-hand panel), we show the spheroid mass as a function of the *K*-band magnitude for the same redshifts as the previous plots, and the same colour-coding. It is immediately apparent that the offset in the colour–magnitude relation turns into an offset in the mass-to-light ratio, non-linearly evolving with redshift. At $z = 3$ the mass–luminosity relation for the M05 and PEGASE runs is again completely separated, touching at the faint blue end and featuring a different slope. The bias in the *K*-band luminosity for a given galaxy mass is more than 1 mag from $z = 3$ to 1, with a scatter that increases with decreasing redshift, and finally converges at later times. For comparison, Fig. 4 (right-hand panel) shows the spheroid mass as a function of the *V*-band magnitude, and it is apparent that there is no bias between the M05 and PEGASE run in this band. This shows that the offset in the mass-to-light ratio visible in the *K* band is entirely due to the TP-AGB phase.

The predicted *K*-band magnitude of an elliptical galaxy of $M \sim 10^{11}$ M$_\odot$ is ~ -26 in the M05 run and ~ -25 in the PEGASE. A difference of more than 1 mag in *K*-band luminosity at redshift 3 is very significant, especially in the hierarchical structure formation picture. To produce a given *K*-band luminosity without the TP-AGB emission, a higher stellar mass is needed, in older stellar populations, and therefore a higher SFR at high z is required in simulations. The amount of time and the number of mergers needed by the hierarchical mechanism to produce old massive galaxies at

$z = 3$ put a serious strain on the limits of the theory. The inclusion of the TP-AGB phase, by shifting the colours redwards, may help to relieve the hierarchical model of the most drastic constraints on the masses of galaxies at high redshifts.

4 DISCUSSION AND CONCLUSIONS

The offset in the predicted colour–magnitude relation, the galaxy colour distribution and their evolution with redshift described in the previous section is dramatic, and is entirely produced by different prescriptions for the input stellar population models. The test galaxy formation model GalICS was run with the same input physics in both cases, ruling out that any feature in the model is responsible for the offset. The results presented here are solid against different semi-analytical model or SPH simulation implementations, as long as the framework in use is the hierarchical growth of structures. The relative contribution of the TP-AGB to the overall galaxy emission mainly depends on the average age of the stellar populations, and therefore is only sensitive to the mass assembly and star formation history. For this reason, we expect similar results with any galaxy formation model based on CDM hierarchical clustering. The details of this offset will depend on individual model recipes, through second-order effects that are expected to be produced by different implementations of cooling and feedback.

The implications of these results have a great impact on the models of structure formation. The redshift-dependent, non-linear offset in the predicted *K*-band luminosities shifts the rest-frame $V - K$ colours redwards and the mass-to-light ratio in the red/infrared downwards, especially for massive galaxies. The key difference lies in producing extremely red $V - K$ colours in not-so-massive, young or intermediate-age galaxies, still actively star forming and possibly very blue in $B - V$, rather than only to old and dead, passively evolving systems.

It has been pointed out that hierarchical clustering is unable to account for the observed red galaxy population at high redshifts (Yan et al. 2004; Cirasuolo et al. 2008). The comparison between observations and simulations needs to be reconsidered in the light of the results presented here. We produce very red optical-to-near-IR colours in young galaxies, without the need of large stellar masses. Simulations would be relieved of the constraint to produce high

SFRs at high redshifts, hard to achieve because the dark matter halo assembly process and the baryonic cooling strain to put together much stellar mass very fast at such early epochs.

We are now set on testing our results to see in how far the new model alleviates the difficulties in the convergence between theoretical predictions and observations. In follow-up papers, we will analyse the impact of our results on key observational tests such as luminosity function, Tully– Fisher relation and the properties of the population of extremely red objects.

REFERENCES

Baugh C. M., 2006, Rep. Prog. Phys., 69, 3101
Bower R. G., Benson A. J., Malbon R., Helly J., Frenk C. S., Baugh C. M., Cole S., Lacey C. G., 2006, MNRAS, 370, 645
Bruzual G. A., 2007, in Vazdekis A., Peletier R., eds, Proc. IAU Symp. 241, Stellar Populations as Building Blocks of Galaxies. Cambridge Univ. Press, Cambridge
Bruzual G. A., Charlot S., 2003, MNRAS, 344, 1000
Cattaneo A., Combes F., Colombi S., Bertin E., Melchior A.-L., 2005, MNRAS, 359, 1237
Cirasuolo M., McLure R. J., Dunlop J. S., Almaini O., Foucaud S., Simpson C., 2008, MNRAS, submitted (arXiv:0804.3471)
Conroy C., Gunn J. E., White M., 2008, ApJ, submitted (arXiv:0809.4261)
Croton D. J. et al., 2006, MNRAS, 365, 11
De Lucia G., Springel V., White S. D. M., Croton D. J., Kauffmann G., 2006, MNRAS, 366, 499
Devriendt J. E. G., Guiderdoni B., Sadat R., 1999, A&A, 350, 381
Eminian C., Kauffman G., Charlot S., Wild V., Bruzual G., Rettura A., Loveday J., 2008, MNRAS, 384, 930
Fioc M., Rocca-Volmerange B., 1997, A&A, 326, 950
Granato G. L., De Zotti G., Silva L., Bressan A., Danese L., 2004, ApJ, 600, 580
Hatton S., Devriendt J. E. G., Ninin S., Bouchet F. R., Guiderdoni B., Vibert D., 2003, MNRAS, 343, 75
Khochfar S., Silk J., Windhorst R. A., Ryan R. E. Jr, 2007, ApJ, 668, L115
Maraston C., 1998, MNRAS, 300, 872
Maraston C., 2005, MNRAS, 362, 799 (M05)
Marigo P., Girardi L., 2007, A&A, 469, 239
Menci N., Fontana A., Giallongo E., Salimbeni S., 2005, ApJ, 632, 49
Monaco P., Fontanot F., Taffoni G., 2007, MNRAS, 375, 1189
Mori M., Umemura M., 2006, Nat, 440, 644
Naab T., Johansson P. H., Ostriker J. P., Efstathiou G., 2007, ApJ, 658, 710
Nagamine K., Cen R., Hernquist L., Ostriker J. P., Springel V., 2005, ApJ, 627, 608
Silva L., Granato G. L., Bressan A., Danese L., 1998, ApJ, 509, 103
Somerville R. S., Hopkins P. F., Cox T. J., Robertson B. E., Hernquist L., 2008, MNRAS, 391, 481
Swinbank A. M. et al., 2008, MNRAS, 391, 420
Yan H. et al., 2004, ApJ, 616, 63

This paper has been typeset from a T_EX/L^AT_EX file prepared by the author.